

# Domain Regularized Transfer Component Analysis

Lei Zhang

College of Communication Engineering  
Chongqing University, Chongqing 400044, China  
leizhang@cqu.edu.cn

Yan Liu

College of Communication Engineering  
Chongqing University, Chongqing 400044, China  
Jolly817@sina.com

**Abstract**—Anti-drift is an emergent and challenging issue in data-related subjects. In this paper, we propose to address the time-varying drift (e.g. electronic nose drift). By viewing drift to be with different probability distribution from the regular data, a robust subspace projection approach with PCA synthesis is proposed for anti-drift. The main idea behind is that given two clusters of data points with different probability distribution caused by drift, we tend to find a latent projection  $P$  (i.e. a group of basis), such that the newly projected subspace of the two clusters is with similar distribution (i.e. anti-drift). The merits of the proposed domain regularized component analysis (DRCA) method are threefold: 1) the proposed subspace projection mechanism is unsupervised, without using any label information of data in anti-drift; 2) a simple but effective concept of domain distance is proposed to represent the mean distribution discrepancy metric; 3) the proposed anti-drift method can be easily solved by Eigen decomposition, and anti-drift is manifested with a well solved projection matrix in real time application. Experiment on a benchmark drift dataset demonstrates the effectiveness of the proposed DRCA method.

**Keywords**—Anti-drift, time-varying drift, electronic nose, component analysis

## I. INTRODUCTION

In olfaction related gas sensing instruments (e.g. electronic nose), sensor drift shows nonlinear dynamic behavior in a multi-dimensional sensor array [1]. Sensor drift effect is caused by many objective factors such as aging, poisoning, and the fluctuations of the ambient environmental variables (e.g. humidity, temperature) [2]. As a result, the instrument responds differently to a constant concentration of some contaminants at different ambient conditions. Drift is once thought to be an ill-posed problem due to the very irregular characteristics.

Electronic nose, as a gas sensing device with pattern recognition unit for artificial olfaction, has witnessed a wide progress in applications, systems and algorithms during the past two decades [3-8]. Pattern recognition algorithms have been widely studied in E-nose for classification and regression [9-11]. Some excellent reviews of the pattern classification and signal processing methods in machine olfaction and E-nose can be referred to as [12-14].

In this paper, we focus on the hot topic of long-term drift in E-nose. Drift is supposed to be some slow, continuous and uncertain effect, which is affecting the classification performance of an E-nose, due to the undesirable “unknown

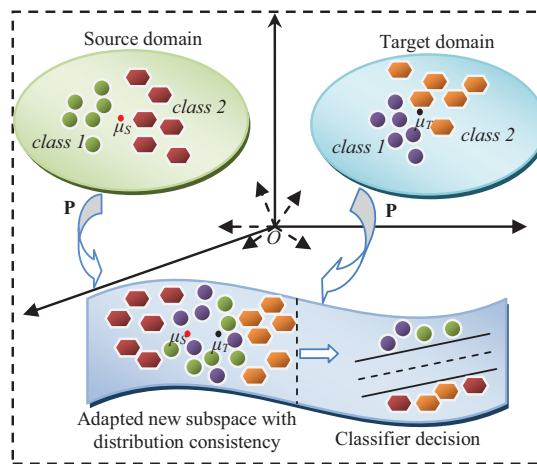


Fig. 1. Schematic diagram of the proposed DRCA method; after a subspace projection  $P$ , the source domain and target domain of different space distribution lie in a latent subspace with good distribution consistency; in this latent subspace, the classification of two classes is successfully achieved.

noise”. Although researchers have proposed many different methods for drift compensation from the angle of ensemble classifiers, semi-supervised learning, drift direction and drift correction, the results are still unsatisfactory [15-20]. From the angle of machine learning, a basic assumption in learning theory is that the probability distribution between the training data and the testing data should be consistent. In this paper, we propose a linear subspace alignment based drift adaptation technique, which tends to achieve drift compensation by removing the distribution discrepancy between the normal E-nose data and the drifted E-nose data.

Under the construction of principal component analysis, we propose a domain regularized component analysis (DRCA) method, which aims at improving the distribution consistency and achieving drift adaptation in principal component subspaces of normal (source domain) and drifted data (target domain). Inspired by transfer learning and domain adaptation [18], we give that the normal data is from *source domain* and the drifted data is from *target domain*. The basic idea of the proposed DRCA method is illustrated vividly in Fig. 1.

## II. RELATED WORK

Recently, many researchers have proposed different methods for handling drift issue of E-nose. Specifically, we

present the existing work from classifier-level and feature level. *In classifier level*, Martinelli *et al.* proposed an artificial immune system based adaptive classifier for drift mitigation [15]. Vergara *et al.* proposed a classifier ensemble model for drift compensation, in which multiple SVMs with weighted ensemble are involved [16]. Zhang *et al.* [17] proposed a domain adaptation extreme learning machine based transfer learning method for drift compensation, in which the classifier is learned with source and target domain simultaneously, by adaptive cross-domain learning. Liu *et al.* [18] also proposed a semi-supervised domain adaptation, in which manifold learning with affinity structure preservation is considered. These methods focus on the robust classifier learning, but neglect the important issue of data distribution mismatch. *In feature level*, Artursson *et al.* proposed a component correction based principal component analysis method, which aims at finding the drift direction and then remove the drift directly from the data [19]. The residual is recognized to be the non-drifted data. These methods suppose that the drift is some additive noise on the data, which may violate the basic property of drift. To our knowledge, it is the first time to address drift problem, by viewing drift to be some distribution bias in feature space between drift and regular data.

### III. THE PROPOSED DRCA METHOD

#### A. Notations

The source and target domain are defined by subscript “S” and “T”, respectively. The training data of source and target domain is denoted as  $X_S \in \mathfrak{R}^{D \times N_S}$ ,  $X_T \in \mathfrak{R}^{D \times N_T}$ , where  $D$  is the number of dimensions,  $N_S$  and  $N_T$  are the number of training samples.

#### B. Problem Formulation

As illustrated in Fig. 1, we aim to learn a basis transformation  $\mathbf{P}$  that maps the original space of source and target data to some subspace, where the feature distributions between the mapped source and target data  $Y_S \in \mathfrak{R}^{d \times N_S}$  and  $Y_T \in \mathfrak{R}^{d \times N_T}$  can be kept similar. Therefore, it is rational to have an idea that the mean distribution discrepancy (MDD) between  $\mathbf{Y}_S$  and  $\mathbf{Y}_T$  is minimized. Simply, the MDD concept is shown by the proposed domain distance, which is defined as the distance between the centers of the two domains. Therefore, the MDD minimization is formulated as

$$\min \|\boldsymbol{\mu}_S - \boldsymbol{\mu}_T\|_2^2 = \min \left\| \frac{1}{N_S} \sum_{i=1}^{N_S} \mathbf{y}_S^i - \frac{1}{N_T} \sum_{j=1}^{N_T} \mathbf{y}_T^j \right\|_2^2 \quad (1)$$

where  $\boldsymbol{\mu}_S$  and  $\boldsymbol{\mu}_T$  represents the centers in the new subspace.

According to the subspace projection, the new representation of source and target data in the lower-dimensional subspace can be formulated as

$$\mathbf{Y}_S = \mathbf{P}^T \mathbf{X}_S = \mathbf{P}^T \begin{bmatrix} \mathbf{x}_S^1, \dots, \mathbf{x}_S^{N_S} \end{bmatrix} = \begin{bmatrix} \mathbf{y}_S^1, \dots, \mathbf{y}_S^{N_S} \end{bmatrix} \quad (2)$$

$$\mathbf{Y}_T = \mathbf{P}^T \mathbf{X}_T = \mathbf{P}^T \begin{bmatrix} \mathbf{x}_T^1, \dots, \mathbf{x}_T^{N_T} \end{bmatrix} = \begin{bmatrix} \mathbf{y}_T^1, \dots, \mathbf{y}_T^{N_T} \end{bmatrix} \quad (3)$$

Therefore, we have  $\mathbf{y}_S^i = \mathbf{P}^T \mathbf{x}_S^i$  and  $\mathbf{y}_T^j = \mathbf{P}^T \mathbf{x}_T^j$ . By substituting (2) and (3) into (1), the minimization problem (1) can be reformulated as

$$\min_{\mathbf{P}} \left\| \frac{1}{N_S} \sum_{i=1}^{N_S} \mathbf{P}^T \mathbf{x}_S^i - \frac{1}{N_T} \sum_{j=1}^{N_T} \mathbf{P}^T \mathbf{x}_T^j \right\|_2^2 \quad (4)$$

For learning such a basis transformation  $\mathbf{P}$  that can minimize the mean distribution discrepancy in (4), we should also ensure that the projection does not distort the data itself, such that much more available information can be kept in the new subspace representation. Therefore, for source data it is rational to maximize the following term,

$$\max_{\mathbf{P}} \text{Tr} \left( \left( \mathbf{P}^T \mathbf{X}_S \right) \left( \mathbf{P}^T \mathbf{X}_S \right)^T \right) = \max_{\mathbf{P}} \text{Tr} \left( \mathbf{P}^T \mathbf{X}_S \mathbf{X}_S^T \mathbf{P} \right) \quad (5)$$

It can be seen that by solving (5), the variance (energy) of the source data in the new subspace is maximized, such that the data cannot be distorted and the most available information in the raw data can be remained.

Similarly, for target domain data, we aim at maximizing the following term

$$\max_{\mathbf{P}} \text{Tr} \left( \left( \mathbf{P}^T \mathbf{X}_T \right) \left( \mathbf{P}^T \mathbf{X}_T \right)^T \right) = \max_{\mathbf{P}} \text{Tr} \left( \mathbf{P}^T \mathbf{X}_T \mathbf{X}_T^T \mathbf{P} \right) \quad (6)$$

In actual application, there is little data in target domain by comparing to the source domain. In order to learn an effective linear subspace  $\mathbf{P}$  for drift adaptation, we propose a target domain regularized variance maximization idea and effectively avoid bias learning. Therefore, the variance maximization formulation shown in Eq.(5) and Eq.(6) can be integrated together by using a trade-off parameter as follows

$$\max_{\mathbf{P}} \text{Tr} \left( \mathbf{P}^T \left( \mathbf{X}_S \mathbf{X}_S^T + \lambda \cdot \mathbf{X}_T \mathbf{X}_T^T \right) \mathbf{P} \right) \quad (7)$$

where  $\lambda$  denotes the trade-off (regularization) parameter.

The proposed target domain regularized component analysis (DRCA) model aims at minimizing the mean distribution discrepancy (MDD) in (4) and maximizing the regularized variance in (7) of source and target data, simultaneously. Therefore, by integrating (4) and (7) together, the proposed DRSA model can be formulated as

$$\max_{\mathbf{P}} \frac{\text{Tr} \left( \mathbf{P}^T \left( \mathbf{X}_S \mathbf{X}_S^T + \lambda \cdot \mathbf{X}_T \mathbf{X}_T^T \right) \mathbf{P} \right)}{\left\| \frac{1}{N_S} \sum_{i=1}^{N_S} \mathbf{P}^T \mathbf{x}_S^i - \frac{1}{N_T} \sum_{j=1}^{N_T} \mathbf{P}^T \mathbf{x}_T^j \right\|_2^2} \quad (8)$$

The maximization problem in Eq.(8) can be re-written as

$$\max_{\mathbf{P}} \frac{\mathbf{P}^T \left( \mathbf{X}_S \mathbf{X}_S^T + \lambda \cdot \mathbf{X}_T \mathbf{X}_T^T \right) \mathbf{P}}{\mathbf{P}^T \left( \boldsymbol{\mu}_S - \boldsymbol{\mu}_T \right) \left( \boldsymbol{\mu}_S - \boldsymbol{\mu}_T \right)^T \mathbf{P}} \quad (9)$$

#### C. Model Optimization

In the maximization problem Eq.(9), there are many possible solutions of  $\mathbf{P}$  (i.e. non-unique solutions). To guarantee the unique property of solution, we impose an equality constraint on the optimization problem, and then Eq.(9) can be written as

**Algorithm 1.** The proposed DRCA**Input:** Source data  $X_S \in \mathfrak{R}^{D \times N_S}$  and target data  $X_T \in \mathfrak{R}^{D \times N_T}$ ,  $\lambda$ ,  $d$ ;**Procedure:**1. Compute the centroid of source data  $\mu_S$ ;2. Compute the centroid of target data  $\mu_T$ ;3. Compute the matrix  $\mathbf{A}$  as

$$\mathbf{A} = \left( (\mu_S - \mu_T)(\mu_S - \mu_T)^T \right)^{-1} \left( X_S X_S^T + \lambda \cdot X_T X_T^T \right)$$

4. Perform the eigenvalue decomposition of  $\mathbf{A}$  by using (13);5. Compute the optimal subspace  $\mathbf{P}^* = [\mathbf{p}_1, \mathbf{p}_2, \dots, \mathbf{p}_d]$  by (14);

6. New subspace projection with drift adaptation by

$$\mathbf{X}'_S = (\mathbf{P}^*)^T X_S \text{ and } \mathbf{X}'_T = (\mathbf{P}^*)^T X_T$$

**Output:** The basis  $\mathbf{P}$  and the drift adapted data.

$$\max_{\mathbf{P}} \mathbf{P}^T \left( X_S X_S^T + \lambda \cdot X_T X_T^T \right) \mathbf{P} \quad (10)$$

$$\text{s.t. } \mathbf{P}^T (\mu_S - \mu_T)(\mu_S - \mu_T)^T \mathbf{P} = \eta$$

where  $\eta$  is a positive constant value.

To solve (10), the Lagrange multiplier function is written as

$$L(\mathbf{P}, \rho) = \mathbf{P}^T \left( X_S X_S^T + \lambda \cdot X_T X_T^T \right) \mathbf{P} - \rho \left( \mathbf{P}^T (\mu_S - \mu_T)(\mu_S - \mu_T)^T \mathbf{P} - \eta \right) \quad (11)$$

where  $\rho$  denotes the Lagrange multiplier coefficient.By setting the partial derivation of  $L(\mathbf{P}, \rho)$  with respect to  $\mathbf{P}$  to be 0, we have

$$\left( (\mu_S - \mu_T)(\mu_S - \mu_T)^T \right)^{-1} \left( X_S X_S^T + \lambda \cdot X_T X_T^T \right) \mathbf{P} = \rho \mathbf{P} \quad (12)$$

From (12), we can observe that the  $\mathbf{P}$  can be obtained by solving the following Eigenvalue decomposition problem,

$$\mathbf{A} \mathbf{P} = \rho \mathbf{P} \quad (13)$$

where  $\mathbf{A} = \left( (\mu_S - \mu_T)(\mu_S - \mu_T)^T \right)^{-1} \left( X_S X_S^T + \lambda \cdot X_T X_T^T \right)$ , and  $\rho$  denotes the diagonal matrix of eigenvalues.From (13), it is clear that  $\mathbf{P}$  denotes the eigen-vectors. Due to that the model (10) is a maximization problem, therefore, the optimal subspace  $\mathbf{P}^*$  denotes the eignvectors with respect to the first  $d$  largest eigenvalues  $[\rho_1, \dots, \rho_d]$  represented by

$$\mathbf{P}^* = [\mathbf{p}_1, \mathbf{p}_2, \dots, \mathbf{p}_d] \quad (14)$$

For easy implementation, the proposed DRSA algorithm is summarized in Algorithm 1.

## IV. EXPERIMENTS

For verification of the proposed DRCA method, the real sensor drift benchmark dataset of three years collected by an E-nose from Vergara *et al.* in UCSD [16] is used in our experiment. The dataset was gathered during the period of 36 months from January 2008 to February 2011 based on a gas delivery platform. The E-nose is with 16 gas sensors, and exposed to six kinds of pure gaseous substances, such as acetone, acetaldehyde, ethanol, ethylene, ammonia, and toluene at different concentration levels. Totally, this dataset contains 13910 measurements (samples), which are divided into 10 batches of time series. In feature extraction, 8 features were extracted for each sensor, and consequently a 128-

dimensional feature vector (16×8) is formulated for each sample. We refer interested readers to as [16] for details.

Due to the distribution inconsistency between batch 1 (training data) and other batches (testing data), the recognition performance of the trained pattern classifier would be degraded, because it violates the basic assumption of machine learning that the training data and testing data should be with the same or similar probability distribution (i.e. independent identical distribution, *i.i.d.*). The essential task for the proposed method is to improve the classification performance. Therefore, the classification accuracy of 6 classes on each batch is reported as evaluation metric. In comparisons, two experimental settings by following [16] are given as follows.

1) *Setting 1:* Take batch 1 as source domain for model training, and test on batch  $K$ ,  $K=2, \dots, 10$  (target domains). The classification accuracy on batch  $K$  is reported.

2) *Setting 2:* Take batch  $K-1$  as source domain for model training, and test on batch  $K$ ,  $K=2, \dots, 10$  (target domains). The classification accuracy on batch  $K$  is reported.

For classification, a multi-class SVM with RBF kernel (SVM-rbf) is used as classifier. In comparisons, we compare the proposed DRCA with two baseline subspace methods such as PCA and LDA trained on source data, and eight state-of-the-art results on this benchmark dataset such as CCPCA, SVM ensemble classifier, SVM-gfk, SVM-comgfk, ML-gfk, ML-comgfk, ELM-rbf, and OSC.

We conducted the experiments on *Setting 1* and *Setting 2*, respectively. The recognition results for different methods under Experimental *Setting 1* are reported in Table I, from which we observe that the proposed DRCA achieves the best classification performance. The average classification accuracy is 77.63%, which is 10% higher than the second best learning method, i.e. ML-comgfk.

Further, by following the experimental *Setting 2*, that is, model training on batch  $K-1$  and test on batch  $K$ , and the results are reported in Table II, from which we can see that the proposed DRCA performs the second best performance (74.2% in average). From the quantitative classification accuracy, the effectiveness and competitiveness of the proposed DRCA model have been clearly demonstrated.

## V. CONCLUSION

In this paper, we propose a domain regularized component analysis (DRCA) model for heterogeneous E-nose application. The method is motivated by transfer learning, and the difference of probability distribution between source data and target data incurs the failure of machine learning in data mining. For learning a common subspace for heterogeneous data, an intuitive idea by regularizing the target domain and minimizing the mean distribution discrepancy (MDD) based domain distance is proposed. Motivated by PCA and the proposed idea, a DRCA model is formulated. The optimization algorithm of the proposed DRCA is also induced. Experiments on synthetic dataset, benchmark sensor drift dataset and sensor drift plus shift dataset demonstrate that the proposed DRCA method outperforms several state-of-the arts methods.

## ACKNOWLEDGMENT

This work was supported in part by National Natural Science Foundation of China (Grant 61401048) and in part by the research fund for Central Universities.

REFERENCES

[1] L. Zhang, F. Tian, S. Liu, L. Dang, X. Peng, and X. Yin, "Chaotic time series prediction of e-nose sensor drift in embedded phase space," *Sensors and Actuators B: Chemical*, vol. 182, pp. 71-79, 2013.

[2] F. Hossein-Babaei and V. Ghafarinia, "Compensation for the drift-like terms caused by environmental fluctuations in the response of chemoresistive gas sensors," *Sensors and Actuators B: Chemical*, vol. 143, pp. 641-648, 2010.

[3] L. Zhang and F. Tian, "Performance Study of Multilayer Perceptrons in a Low-Cost Electronic Nose," *IEEE Transactions on Instrumentation and Measurement*, vol. 63, no. 7, pp. 1670-1679, 2014.

[4] L. Zhang and F.C. Tian, "A new kernel discriminant analysis framework for electronic nose recognition," *Analytica Chimica Acta*, vol. 816, pp. 8-17, 2014.

[5] X. Yin, L. Zhang, F. Tian, and D. Zhang, "Temperature Modulated Gas Sensing E-nose System for Low-cost and Fast Detection," *IEEE Sensors Journal*, vol. 16, no. 2, pp. 464-474, 2016.

[6] F. Herrero-Carrón, D.J. Yáñez, F. de Borja Rodríguez, and P. Varona, "An active, inverse temperature modulation strategy for single sensor odorant classification," *Sensors and Actuators B: Chemical*, vol. 206, pp. 555-563, 2015.

[7] F. Hossein-Babaei and A. Amini, "Recognition of complex odors with a single generic tin oxide gas sensor," *Sensors and Actuators B: Chemical*, vol. 194, pp. 156-163, 2014.

[8] M. Palit, B. Tudu, P.K. Dutta, A. Dutta, A. Jana, J. Kumar Roy, N. Bhattacharyya, R. Bandyopadhyay, and A. Chatterjee, "Classification of Black Tea Taste and Correlation With Tea Taster's Mark Using Voltammetric Electronic Tongue," *IEEE Transactions on Instrumentation and Measurement*, vol. 59, no. 8, pp. 2230-2239, 2010.

[9] I. Rodríguez-Lujan, J. Fonollosa, A. Vergara, M. Homer, R. Huerta, "On the calibration of sensor arrays for pattern recognition using the minimal number of experiments," *Chemometrics and Intelligent Laboratory Systems*, vol. 130, pp. 123-134, 2014.

[10] S.K. Jha, K. Hayashi, and R.D.S. Yadava, "Neural, fuzzy and neuro-fuzzy approach for concentration estimation of volatile organic compounds by surface acoustic wave sensor array," *Measurement*, vol. 55, pp. 186-195, 2014.

[11] S.J. Dixon and R.G. Brereton, "Comparison of performance of five common classifiers represented as boundary methods: Euclidean Distance to Centroids, Linear Discriminant Analysis, Quadratic Discriminant Analysis, Learning Vector Quantization and Support Vector Machines, as dependent on data structure," *Chemometrics and Intelligent Laboratory Systems*, vol. 95, pp. 1-17, 2009.

[12] S. Marco and A. Gutiérrez-Gálvez, "Signal and Data Processing for Machine Olfaction and Chemical Sensing: A Review," *IEEE Sensors Journal*, vol. 12, no. 11, pp. 3189-3214, 2012.

[13] F. Röck, N. Barsan, and U. Weimar, "Electronic Nose: Current Status and Future Trends," *Chem. Rev.*, vol. 108, pp. 705-725, 2008.

[14] S.M. Scott, D. James, and Z. Ali, "Data analysis for electronic nose systems," *Microchim Acta*, vol. 156, pp. 183-207, 2007.

[15] E. Martinelli, G. Magna, S. De Vito, R. Di Fuccio, G. Di Francia, A. Vergara, and C. Di Natale, "An adaptive classification model based on the Artificial Immune System for chemical sensor drift mitigation," *Sensors and Actuators B: Chemical*, vol. 177, pp. 1017-1026, 2013.

[16] A. Vergara, S. Vembu, T. Ayhan, M.A. Ryan, M.L. Homer, and R. Huerta, "Chemical gas sensor drift compensation using classifier ensembles," *Sensors and Actuators B: Chemical*, vol. 167, pp. 320-329, 2012.

[17] L. Zhang and D. Zhang, "Domain Adaptation Extreme Learning Machines for Drift Compensation in E-nose Systems," *IEEE Transactions on Instrumentation and Measurement*, vol. 64, no. 7, pp. 1790-1801, 2015.

[18] Q. Liu, M. Ye, S.S. Ge, and X. Du, "Drift Compensation for Electronic Nose by Semi-Supervised Domain Adaption," *IEEE Sensors Journal*, vol. 14, no. 3, pp. 657-665, 2014.

[19] T. Artursson, T. Eklov, I. Lundstrom, P. Martensson, M. Sjostrom, and M. Holmberg, "Drift correction for gas sensors using multivariate methods," *J. Chemometrics*, vol. 14, no. 5-6, pp. 711-723, 2000.

TABLE I  
RECOGNITION ACCURACY (%) UNDER EXPERIMENTAL SETTING 1

Batch ID	Batch 2	Batch 3	Batch 4	Batch 5	Batch 6	Batch 7	Batch 8	Batch 9	Batch 10	Average
PCASVM	82.40	84.80	80.12	75.13	73.57	56.16	48.64	67.45	49.14	<b>68.60</b>
LDA <sub>SVM</sub>	47.27	57.76	50.93	62.44	41.48	37.42	68.37	52.34	31.17	49.91
CC-PCA	67.00	48.50	41.00	35.50	55.00	31.00	56.50	46.50	30.50	45.72
SVM-rbf	74.36	61.03	50.93	18.27	28.26	28.81	20.07	34.26	34.47	38.94
SVM-gfk	72.75	70.08	60.75	75.08	73.82	54.53	55.44	69.62	41.78	63.76
SVM-comgfk	74.47	70.15	59.78	75.09	73.99	54.59	55.88	70.23	41.85	64.00
ML-rbf	42.25	73.69	75.53	66.75	77.51	54.43	33.50	23.57	34.92	53.57
ML-comgfk	80.25	74.99	78.79	67.41	77.82	<b>71.68</b>	49.96	50.79	53.79	67.28
ELM-rbf	70.63	66.44	66.83	63.45	69.73	51.23	49.76	49.83	33.50	57.93
OSC	88.10	66.71	54.66	53.81	65.13	63.71	36.05	40.21	40.08	56.50
<b>DRCA</b>	<b>89.15</b>	<b>92.69</b>	<b>87.58</b>	<b>95.94</b>	<b>86.52</b>	60.25	<b>62.24</b>	<b>72.34</b>	<b>52.00</b>	<b>77.63</b>

TABLE II  
RECOGNITION ACCURACY (%) UNDER EXPERIMENTAL SETTING 2

Batch ID	1→2	2→3	3→4	4→5	5→6	6→7	7→8	8→9	9→10	Average
PCASVM	82.40	<b>98.87</b>	83.23	72.59	36.70	74.98	58.16	84.04	30.61	69.06
LDA <sub>SVM</sub>	47.27	46.72	70.81	85.28	48.87	75.15	77.21	62.77	30.25	60.48
SVM-rbf	74.36	87.83	90.06	56.35	42.52	83.53	<b>91.84</b>	62.98	22.64	68.01
SVM-gfk	72.75	74.02	77.83	63.91	70.31	77.59	78.57	86.23	15.76	68.56
SVM-comgfk	74.47	73.75	78.51	64.26	69.97	77.69	82.69	85.53	17.76	69.40
ML-rbf	42.25	58.51	75.78	29.10	53.22	69.17	55.10	37.94	12.44	48.17
ML-comgfk	80.25	<b>98.55</b>	84.89	<b>89.85</b>	<b>75.53</b>	<b>91.17</b>	61.22	<b>95.53</b>	<b>39.56</b>	<b>79.62</b>
ELM-rbf	70.63	40.44	64.16	64.37	72.70	80.75	88.20	67.00	22.00	63.36
<b>DRCA</b>	<b>89.15</b>	98.11	<b>95.03</b>	69.54	50.87	78.94	65.99	84.04	36.31	<b>74.22</b>